Looking for bimodal distributions in multi-fragmentation reactions

F. Gulminelli

Looking for bimodal distributions in multi-fragmentation reactions

F. Gulminelli

LPC (IN2P3-CNRS/Ensicaen et Université), F-14076 Caen cédex, France[∗]

The presence of a phase transition in a finite system can be deduced, together with its order, from the shape of the distribution of the order parameter. This issue has been extensively studied in multifragmentation experiments, with results that do not appear fully consistent. In this paper we discuss the effect of the statistical ensemble or sorting conditions on the shape of fragment distributions, and propose a new method, which can be easily implemented experimentally, to discriminate between different fragmentation scenarii. This method, based on a reweighting of the measured distribution to account for the experimental constraints linked to the energy deposit, is tested on different simple models, and appears to provide a powerful discrimination.

I. INTRODUCTION

At the transition point of a first order phase transition, the distribution of the order parameter in the corresponding finite system presents a characteristic bimodal behavior in the canonical or grancanonical ensemble[1, 2, 3, 4]. The bimodality comes from an anomalous convexity of the underlying microcanonical entropy. It physically corresponds to the simultaneous presence of two different classes of events, which at the thermodynamic limit leads to phase coexistence. Such behavior is very different from the signal of a second order phase transition, or more generally a critical behavior. In this latter case the order parameter distribution is generally wide but always monomodal, it fulfills specific scaling properties with increasing system size, and presents non-gaussian tails[5].

In the case of nuclear multi-fragmentation, the most natural observable to analyze as a potential order parameter is the size of the heaviest cluster produced in each collision event. Indeed this observable is known to provide an order parameter for a large class of transitions or critical phenomena involving complex clusters, from percolation to gelation, from reversible to irreversible aggregation[5]. Moreover it is reasonable to believe that the largest cluster size is always well correlated to the total energy deposit; this means that it will take different values in the two phases of any transition involving a finite latent heat, thus serving as an order parameter. Many different indications exist[6, 7] that multi-fragmentation may be the finite size and possibly out-of-equilibrium realization of the liquid-gas phase transition of infinite nuclear matter. Also in this case the heaviest cluster size is expected to play the role of an order parameter, because of its good correlation with the system density, as shown by the numerical simulation of the liquid-gas transition[4].

These ideas have been recently applied by the INDRA collaboration to different intermediate-energy heavy-ion collisions data sets, with the aim of tracking the multi-fragmentation phase transition and possibly determining its order[8, 9, 10, 11, 12, 13, 14]. A systematic analysis of different data from central collisions[14] reveals that the heaviest fragment distributions are never bimodal, neither they present the non-gaussian tails that would allow to identify a critical phenomenon. The situation is different in peripheral collisions[9]. In this case, the quasi-projectile heaviest residues are sorted in centrality bins measured from the transverse energy of light charged particles detected on the quasi-target side. The resulting distributions clearly show two different event families when plotted against the asymmetry between the two heaviest fragments $Z_{asy} = (Z_{max} - Z_{second})/(Z_{max} + Z_{second})$, and do not fulfill the scaling properties shown by central collisions. The widths of the two partial distributions are too large for a bimodality to appear in the projection over the Z_{max} axis, but a clear bimodality is seen in the closely correlated Z_{asy} distribution.

The characteristics and order of the nuclear multi-fragmentation transition are thus not completely clear.

It is certainly possible that two very different fragment formation mechanisms act in central and peripheral collisions[15]. It is however also important to note that the sorting conditions are not the same in the different collisions, and the shape of the distributions is obviously influenced by the constraints imposed by the sorting.

In this paper we analyze the effect of the sorting, and propose a new method to detect a possible first order phase transition independent of the mechanism of energy deposit, and without the artificial assumption of a heat bath. Indeed the dependence on the sorting is a manifestation of the statistical mechanics concept of ensemble inequivalence, as we develop in detail below. Working out the relations between the different ensembles will allow us

---

to predict the transformation to apply to the bimodality signal, in order to account for the experimental constraints.
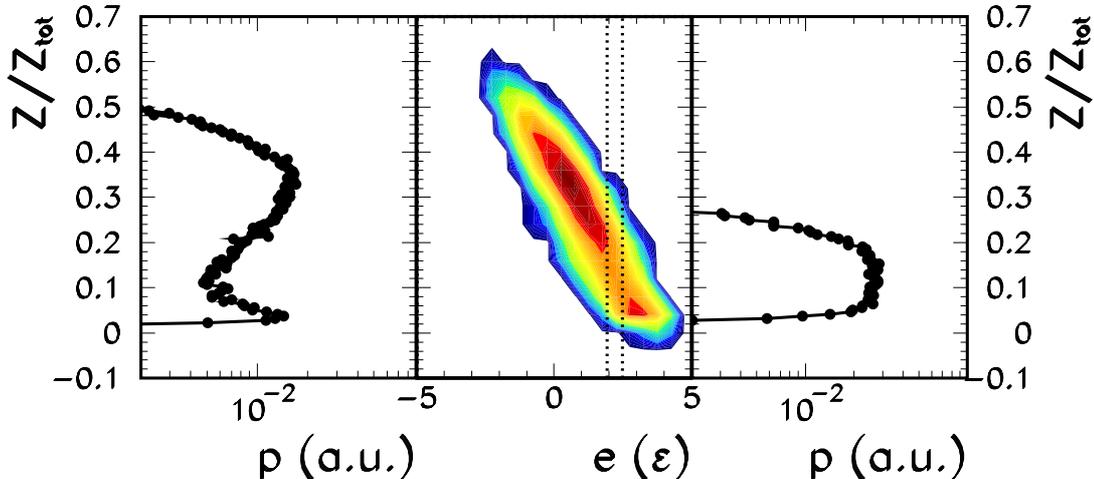
II.   BIMODALITIES AND ENSEMBLES

FIG. 1: *Event distributions in the isobar lattice gas model. A system of 216 particles is considered at a subcritical pressure and a temperature close to the transition temperature. Central panel: canonical distribution in the largest cluster size and energy plane. The left and right figures give the projection of this correlation over the largest cluster size axis. Left: canonical ensemble; right: narrox constraint on the total energy as indicated by the two vertical lines of the central panel. Energy is given in units of the closest neighbors coupling.*

Observables distributions depend on the criterium used to collect the events, i.e. on the statistical ensemble. Concerning the issue of bimodality, a system experiencing a first order phase transition presents a bimodal distribution of its order parameter if and only if the associated observable is constrained only in average through a conjugated Lagrange parameter, and it is not fixed by a conservation law[3, 4, 16].

For example, the energy distribution of a finite system, presenting in the thermodynamic limit a finite-latent-heat phase transition, is bimodal in the canonical ensemble[2, 17]. The same is true for any other observable Z presenting a non-zero correlation with the total energy. If the correlation is loose and the system is small, each of the two peaks may have a large width, which may extend over values characteristic of the other phase, and mask the bimodality. However, the distance between the two peaks Z_1 and Z_2 scales linearly with the number of particles: $(Z_1 - Z_2) \propto N$, while the width of each peak scales only with its square-root: $\sigma_Z \propto \sqrt{N}$, meaning that a bimodal behavior will be recovered in the Z observable, for sufficiently large systems.

In the microcanonical ensemble, the energy distribution is by definition a δ-function, and obviously cannot be bimodal. The distribution of any other observable Z will in general present a finite width, but if the correlation with the energy is strong, the bimodality will be lost. These general arguments are applied to the liquid-gas phase transition in Fig.1, which shows the event distribution of the Lattice Gas Model in the canonical isobar ensemble[4] at the transition temperature. This model presents a transition with finite latent heat between a high density liquid and a low density gas. The order parameter of the liquid-gas transition is known too be one-dimensional, meaning that energy and density, or equivalently volume $V \propto \sum_i r_i^3$, have to be correlated.

This intuitive statement can be formalized in the framework of quantum statistical mechanics[18, 19]. Indeed the result of the statistical measurement of any observable Z, associated to the operator $\hat{Z}$ is

$$< \hat{Z} >_{\hat{D}} = \mathrm{Tr}\hat{Z}\hat{D}, \tag{1}$$

where $\hat{D}$ is the density matrix and Tr means the trace over the quantum Fock or Hilbert space. In the space of Hermitian matrices, the trace provides a scalar product [18]

$$<< \hat{Z}||\hat{D} >> = \mathrm{Tr}\hat{Z}\hat{D}. \tag{2}$$

It is then possible to define an orthonormal basis of Hermitian operators $\{\hat{Z}_l\}$ in the observables space, and to interpret the measurement $<\hat{Z}_l>_{\hat{D}}$ as the projection of the density matrix over the corresponding axis. Statistically independent observations can thus be associated to orthogonal observables in the Liouville space.

As a practical consequence, in the liquid-gas phase transition the distribution at the transition temperature must be bimodal both in the volume and in the energy direction[4]. As anticipated in the introduction, the size of the largest cluster is also correlated to both volume and energy, and as such it can be used as an equivalent order parameter. This is shown in the left side of Fig.1: at the transition temperature, the distribution of the largest-cluster size shows two peaks separated by a region of convexity. These observations are done in the canonical ensemble. If energy is constrained as in the microcanonical ensemble, the two phases are not accessible in the same ensemble of events any more, and bimodality is lost. This is not only true for the exact energy conservation implied by the microcanonical ensemble, but for any strong constraint on the energy. This is shown in the right side of Fig.1: the distribution issued from a narrow energy constraint on the canonical event set is a normal distribution.

III. BIMODALITIES AND CONVEXITY ANOMALIES

This behavior is a consequence of ensemble inequivalence, which has been addressed by numerous works in the literature[20]. In particular the presence of a conservation constraint on an order parameter has been reported to modify different phase transition observables, making a first order transition look like a continuous one[16, 21, 22].

The prototype of an ensemble constraining the order parameter is the microcanonical ensemble. There, the phase transition can be univocally recognized studying the curvature properties of the density of states[23]. Indeed from the standard definition of the canonical ensemble

$$p_\beta(E) = W(E)\exp(-\beta E)Z_\beta^{-1} \tag{3}$$

we can immediately see that a bimodality in the canonical energy distribution is exactly equivalent to a convex intruder in the microcanonical entropy $S = \log W$, which leads to the well known microcanonical negative heat capacity[4, 23]. Let us now consider the case of a second observable Z. If both E and Z are order parameters, and the transition is first order, the two-dimensional probability distribution $p(E, Z)$ should be bimodal in both the E and the Z direction within the ensemble where the observables are fixed by the conjugated Lagrange multipliers β, λ [3]:

$$p_\beta(E, Z) = W(E, Z)\exp(-\beta E - \lambda Z)Z_{\beta,\lambda}^{-1} \tag{4}$$

All conservation laws on other variables are implicitly accounted in the definition of the density of states W. For instance, if Z represents the largest cluster size and the total system size is Z_{tot}, W reads

$$W(E, Z) = W_{Z_{tot}}(E, Z) = \sum_{(n)} \delta(E - E^{(n)})\delta(Z - Z^{(n)})\delta(Z_{tot} - Z_{tot}^{(n)}) \tag{5}$$

where the sum extends over the system microstates. The search for bimodalities can only be done in this (extended) canonical ensemble, and is exactly equivalent to the study of the curvature matrix of the entropy in the two-dimensional observable space

$$C = \begin{pmatrix} \partial^2 S/\partial E^2 & \partial^2 S/\partial E \partial Z \\ \partial^2 S/\partial Z \partial E & \partial^2 S/\partial Z^2 \end{pmatrix} \tag{6}$$

If this curvature matrix has two positive eigen-values, this means that and Z and E are associated to two independent order parameters. In the more physical case of a one-dimensional order parameter, only one eigen-value is positive, and the associated eigen-vector can be taken as the "'best"' order parameter. It is the linear combination of the E and Z observables, which gives the best separation of the two phases in the two-dimensional space[2].

In the physical case of nuclear multi-fragmentation experimentally studied through nuclear collisions, the distribution of the deposited energy crucially depends on the entrance channel dynamics and data selection criteria. In the case of quasi-projectile events selected in heavy ion collisions, the energy distribution is very large, and is determined by the impact parameter geometry and dissipation dynamics. If events are sorted in centrality bins, the distribution is centered on a well defined value given by the average dissipation at the considered impact parameter, but the distribution has a finite width that depends in a non-controlled way on the selection criteria. The statistical ensemble describing multi-fragmentation data is thus neither canonical nor microcanonical, and should rather be described in terms of the gaussian ensemble[25], which gives a continuous interpolation between canonical and microcanonical. If E and Z have a non zero correlation as we expect , $W(E, Z) \neq W_E(E)W_Z(Z)$, the distribution of energy will affect

also the distribution of Z, and the concavity of the Z distribution will not be univocally linked to the concavity of the entropy.

Concerning the explicit constraint λ on Z, there is no reason to believe that the collision dynamics or the data treatment induces a specific constraint on the size of the largest cluster, other than the total mass and charge conservation, which are already implemented in the definition of the state density. This means that we will consider in the following $\lambda = 0$.

IV. RELYING OBSERVABLES DISTRIBUTIONS TO THE UNDERLYING ENTROPY

In the last section we have argued that, in the absence of a canonical sorting, there is no one-to-one correspondence between the shape of the probability distribution and the phase transition properties of the system implied by its density of states. This is not only true for the energy, but also for all other observables that present a non-zero correlation with the energy. Unfortunately, if the order parameter is one-dimensional, all observables that can be proposed to study bimodality (charge of the heaviest cluster, asymmetry, etc..) must be correlated with the energy. This means that the presence (or absence) of the bimodality signal may depend on the experimental sorting conditions.

It is however important to note that if the energy distribution cannot be experimentally controlled, it can be - at least approximately - a-posteriori measured. This means that it is possible to unfold from the experimental distribution the contribution of the entropy, giving the phase properties of the system, and the contribution of the energy distribution, which depends on the collision dynamics. Indeed, as long as no explicit bias acts on the Z variable, the experimental distribution can be calculated from the canonical one eq.(4) by a simple reweighting of the probabilities associated to each deposited energy

$$p_{exp}(E, Z) = p_\beta(E, Z) \frac{p_{exp}(E)}{p_\beta(E)} \tag{7}$$

where $p_{exp}(E)$ is the measured energy distribution.

In the following, we explicit the effect of this experimental bias in the two cases of interest: an entropy curvature matrix with two negative eigen-values, corresponding to the absence of a phase transition, and an entropy presenting one direction of convexity (first order phase transition).
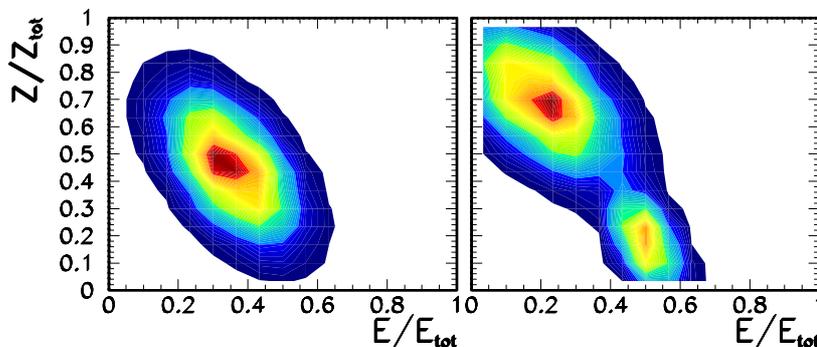
A. The monomodal case

FIG. 2: *Canonical distributions in the plane of the total thermal energy, normalized to the total available energy, and the size of the largest cluster, normalized to the total system size, in the (double) saddle point approximation. Right part: case of a first order phase transition eq.(20). Left part: without transition, eq.(9). The corresponding parameters are given in the text.*

Let us consider again the density of states $W(E, Z) = \exp(S(E, Z))$ in the two-dimensional observable space defined by the total energy E and the largest cluster size Z. In the absence of a phase transition, this function is concave everywhere. To evaluate the partition sum at a temperature β^{-1} we can make a saddle point approximation

$$S(E, Z) = S_0 + \beta(E - E_\beta) - c_{11}(E - E_\beta)^2 - c_{22}(Z - Z_\beta)^2 + c_{12}(E - E_\beta)(Z - Z_\beta) \tag{8}$$

where E_β, Z_β are the most probable values of E and Z at a temperature β^{-1}, and $C = \{c_{ij}\}$ is the entropy curvature matrix eq.(6). In this approximation the event distribution is a gaussian

$$p_\beta(E, Z) = \frac{1}{2\pi} \frac{1}{\sqrt{det\Sigma}} \exp\left(-\frac{1}{2}\vec{x}\Sigma^{-1}\vec{x}\right) \tag{9}$$

where $\vec{x} = (E - E_\beta, Z - Z_\beta)$, and the variance-covariance matrix Σ is related to the curvature matrix by

$$\frac{1}{2(1 - \rho^2)\sigma_E^2} = c_{11} = -\frac{1}{2}\frac{\partial^2 S}{\partial E^2}\Big|_{E_\beta} \tag{10}$$

$$\frac{1}{2(1 - \rho^2)\sigma_Z^2} = c_{22} = -\frac{1}{2}\frac{\partial^2 S}{\partial Z^2}\Big|_{Z_\beta} \tag{11}$$

$$\frac{\rho}{(1 - \rho^2)\sigma_E\sigma_Z} = c_{12} = c_{21} = \frac{1}{2}\frac{\partial^2 S}{\partial E\partial Z}\Big|_{E_\beta, Z_\beta} \tag{12}$$

An example is given in the left part of Figure 2. To fix the ideas we have chosen $E_\beta = 0.35E_{tot}$, $Z_\beta = 0.45Z_{tot}$, $\sigma_E = 0.1E_{tot}$, $\sigma_Z = 0.15Z_{tot}$, $\rho = -0.6$, where E_{tot} and Z_{tot} are the total available energy and size, respectively. The inclusive probabilities associated to this distribution, or marginal distributions, are simple gaussians

$$p_\beta(E) = \frac{1}{\sqrt{2\pi\sigma_E^2}} \exp\left(-\frac{(E - E_\beta)^2}{2\sigma_E^2}\right) \tag{13}$$

$$p_\beta(Z) = \frac{1}{\sqrt{2\pi\sigma_Z^2}} \exp\left(-\frac{(Z - Z_\beta)^2}{2\sigma_Z^2}\right) \tag{14}$$

$$\tag{15}$$

Deviations from a perfect gaussian are in principle possible because of the effect of the boundary, which limits the possible values of E and Z due to the conservation laws. These effects are however very small in all physical cases of interest, and the marginal distributions are largely independent of the correlation coefficient.
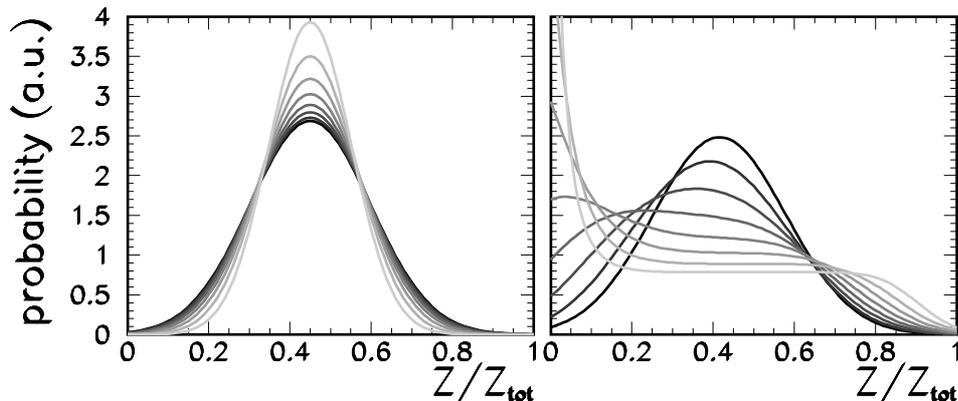

FIG. 3: *Marginal distribution for the monomodal case represented in the left part of Figure 2. Left: gaussian ensemble eq.(7). Right: reweighted distribution eq.(24). The correlation coefficient is varied from $\rho = -0.15$ (black lines) to $\rho = -0.85$ (lightest grey). The other parameters are taken as for Figure 2.*

As we have stressed in the previous section, in the experimental case, because of the absence of an external heat bath, there is no reason to believe that the event distribution can be described by eq.(9). Even if the partitions may fully explore the available phase space, the dynamics of the entrance channel plus the detection and sorting constraints will lead to an energy distribution which is not uniquely characterized by its average value $< E >$. When data are sorted in centrality bins, the energy distributions as measured from calorimetric algorithms are generally close to gaussians. This can be easily understood in the framework of information theory[24], where such a situation can be dealt with introducing the energy variance as a second constraint, which naturally leads to the gaussian ensemble[25]. Therefore we will take as a typical shape for $p_{exp}(E, Z)$ the form (7) where $p_{exp}(E)$ is a gaussian of average E_{exp} and variance σ_{exp}^2. This choice is only done to present some realistic numerical applications, and is readily extended to more general situations.

Eq.(9) and eq.(7) have the same functional dependence, with an important difference though. In the case of eq.(9) the first two moments of the energy distribution eq.(13) are directly related to the canonical partition sum $\ln Z_\beta$ by

$$E_\beta = -\frac{\partial \ln Z_\beta}{\partial \beta} \tag{16}$$

$$C\beta^{-2} = \sigma_E^2 = \frac{\partial^2 \ln Z_\beta}{\partial \beta^2} \tag{17}$$

and, in the saddle point approximation, to the microcanonical temperature T and heat capacity C_μ

$$T^{-1} = \frac{\partial S(E, Z)}{\partial E}|_{E_\beta} \tag{18}$$

$$\frac{1}{(1-\rho^2)\sigma_E^2} = \frac{1}{C_\mu T^2} = -\frac{\partial^2 S(E, Z)}{\partial E^2}|_{E_\beta}. \tag{19}$$

On the other hand, the first two moments of the energy distribution (7) are external constraints imposed by the collision dynamics, that have a priori no direct connection with thermodynamics. Since the folding of gaussians is still a gaussian, the corresponding Z distributions, shown for the model case discussed above in the left part of Figure 3, are also of gaussian shape. The width of the distribution depends on the value of the correlation coefficient ρ (a lower value of the correlation leading to a larger distribution), and all distributions are normal. For the specific application of Figure 3, we have fixed $E_{exp} = E_\beta$, $\sigma_{exp} = \sigma_E/2$.

These observations mean that, if the system does not present a phase transition, the non-canonical experimental sorting does not qualitatively bias the shape of the measured Z distribution.
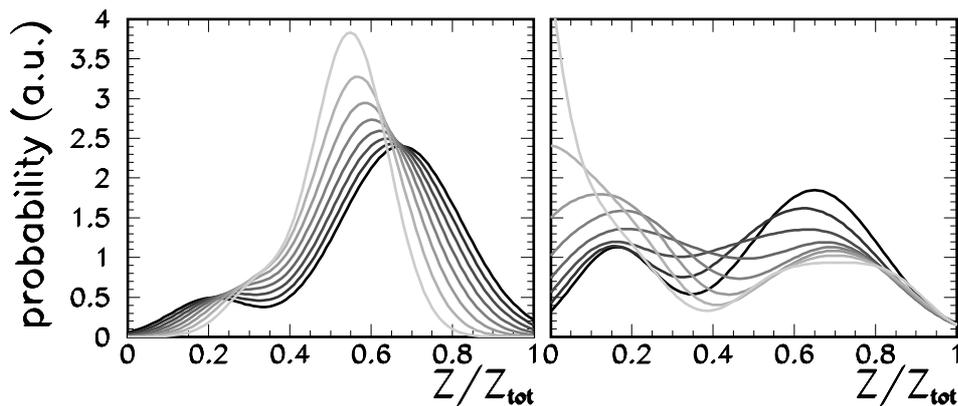
B.   The bimodal case

FIG. 4: *Marginal distribution for the bimodal case represented in the right part of Figure 2. Left: gaussian ensemble eq.(22). Right: reweighted distribution eq.(24). The correlation coefficient is varied from $\rho = -0.15$ (black lines) to $\rho = -0.85$ (lightest grey). The other parameters are taken as for Figure 2.*

In the presence of a first order phase transition with a finite latent heat, the saddle point approximation eq.(8) fails[23]. If the system is not too small, a double saddle point approximation around the two maxima (E_l, Z_l), (E_g, Z_g) can however be employed [3], leading to a double humped distribution

$$p_\beta(E, Z) = N_l \frac{1}{\sqrt{det\Sigma_l}} \exp\left(-\frac{1}{2}\vec{x_l}\Sigma_l^{-1}\vec{x_l}\right) + N_g \frac{1}{\sqrt{det\Sigma_g}} \exp\left(-\frac{1}{2}\vec{x_g}\Sigma_g^{-1}\vec{x_g}\right) \tag{20}$$

where $\vec{x_i} = (E - E_i, Z - Z_i)$, $i = l, g$, Σ_l (Σ_g) represent the variance-covariance matrix evaluated at the liquid (gas) solution, and $N_l(\beta)$, $N_g(\beta)$ are the proportions of the two phases , with $N_l\sqrt{det\Sigma_g} = N_g\sqrt{det\Sigma_l}$ at the transition temperature β_t. An example of a distribution at β_t is given in the right part of Figure 2. To fix the ideas we have chosen $E_l = 0.2E_{tot}$, $Z_l = 0.7Z_{tot}$, $\sigma_{El} = 0.12E_{tot}$, $\sigma_{Zl} = 0.15Z_{tot}$, $E_g = 0.5E_{tot}$, $Z_g = 0.18Z_{tot}$, $\sigma_{Eg} = 0.05E_{tot}$, $\sigma_{Zg} = 0.1Z_{tot}$, $\rho_l = \rho_g$.

If the distance in the Z direction between the two phases $Z_l - Z_g$ is sufficiently large respect to the associated variances σ_{Zl}, σ_{Zg}, as it is the case in Fig.2, the presence of the transition can then be inferred looking for the temperature interval associated to a bimodal shape of the Z distribution[2]

$$p_\beta(Z) = N_l \sqrt{\frac{2\pi}{\sigma_{Zl}^2}} \exp\left(-\frac{(Z-Z_l)^2}{2\sigma_{Zl}^2}\right) + N_g \sqrt{\frac{2\pi}{\sigma_{Zg}^2}} \exp\left(-\frac{(Z-Z_g)^2}{2\sigma_{Zg}^2}\right) \tag{21}$$

If we do not dispose of a canonical sample however the situation is not so simple. Let us consider the case where the experimental energy distribution belongs to the gaussian ensemble with an average E_{exp} and a variance σ_{exp}^2 which can be experimentally measured for each given sorting. Then the measured Z distribution reads (taking $\rho_l = \rho_g$):

$$p_{exp}(Z) \propto \int_{E_{min}}^{E_{max}} dE\, p_{\beta_t}(E,Z) \frac{\exp\left(-\frac{(E-E_{exp})^2}{2\sigma_{exp}^2}\right)}{\frac{\sigma_{Zl}}{\sigma_{El}\sigma_{Zl}+\sigma_{Eg}\sigma_{Zg}}\exp\left(-\frac{(E-E_l)^2}{2\sigma_{El}^2}\right) + \frac{\sigma_{Zg}}{\sigma_{El}\sigma_{Zl}+\sigma_{Eg}\sigma_{Zg}}\exp\left(-\frac{(E-E_g)^2}{2\sigma_{Eg}^2}\right)} \tag{22}$$

which may look close to gaussian even in the phase transition region. In particular if the energy distribution is not very large, the sample corresponding to the transition energy E_t (i.e. the energy corresponding to the minimum probability of eq.(20)) will not explore the energy domains corresponding to the liquid $E \approx E_l \pm \sigma_{El}$ and to the gas phase $E \approx E_g \pm \sigma_{Eg}$. If Z is well correlated to E as we expect, then the only size partitions explored at the transition energy will be the intermediate ones between the liquid and the gas, leading to a normal Z distribution. This can be clearly seen in the left part of Fig.4. Only for very low values of the correlation coefficient the presence of the two phases can be recognized from the Z distribution, where the minimal value for ρ depends on the width of the inclusive energy distribution in the specific experimental situation under study.

V. REWEIGHTING THE ENERGY DISTRIBUTION

In order to recover the information on the concavity of the entropy from the measured distribution eq.(22), we have to get rid of the dominant energy dependence $p_{exp}(E)$. To this aim we can reweight the total (E, Z) distribution in such a way that the total energy distribution is a constant between E_{min} and E_{max}, with $E_{min} < E < E_{max}$, and E_{min}, E_{max} are chosen large enough, such that the spanned energy interval contains the two phases. This procedure corresponds to introducing a weight for each E bin

$$w(E) = \left(\int_0^{Z_{max}} dZ\, p_{exp}(E,Z)\right)^{-1} \tag{23}$$

and generates a new weighted distribution which is a direct measure of the density of states:

$$p_w(E,Z) = \frac{p_{\beta_t}(E,Z)}{p_{\beta_t}(E)} = \frac{W(E,Z)}{W(E)}. \tag{24}$$

In the limiting case of a perfect (anti)correlation between E and Z, the concavity anomaly in the two-dimensional entropy $S(E,Z)$ is solely due to the convex intruder in the function $S(E)$. In this case the order parameter is aligned with the E direction, and it is clear that the reweighted distribution eq.(24) will be a normal distribution in spite of the presence of a first order phase transition. However, in the case of the liquid gas phase transition we have good reasons to expect[26] the order parameter in the enthalpy $H = E + pV$ direction. Since Z is correlated to the volume as well as to the energy, then we may expect a non zero component of the order parameter along the Z axis, and an imperfect correlation between Z and E. In this case an anomaly in $S(E,Z)$ may persist even after subtraction of the entropy $S(E)$, and this anomaly will be shown by a residual bimodality in the distribution (24).

A. Application to model cases

The projections of p_w in the Z direction are shown in a perfectly monomodal and perfectly bimodal case, in the right parts of Figs.3 and 4 respectively. If the underlying entropy presents a convex intruder (Fig.4), the bimodality persists in the reweighted distribution for all considered values of the correlation coefficient. The case of a normal distribution is explored in Fig.3: the distribution is still approximately gaussian if the correlation coefficient is small,
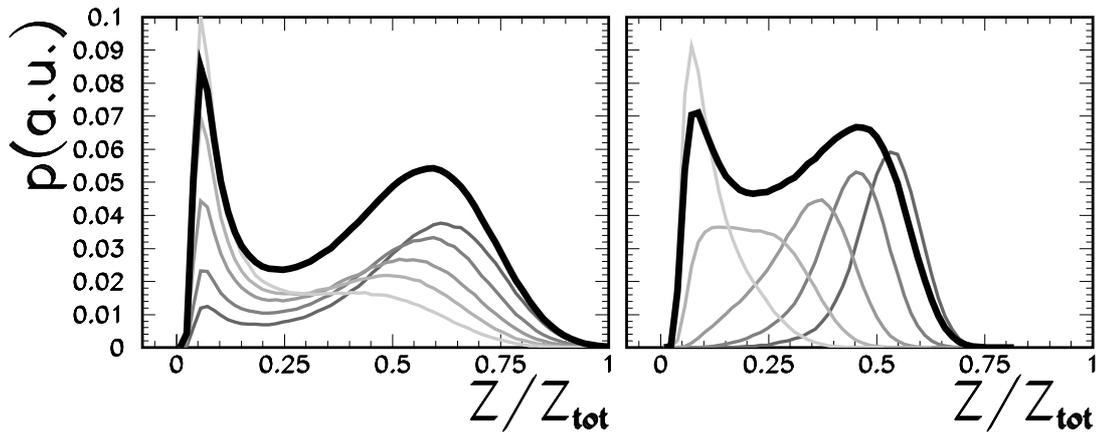
FIG. 5: *Distributions of the size of the largest cluster for a system of N=216 particles within the isobar lattice gas model at subcritical pressure. Left: canonical calculations at temperatures T = 3.72, 3.74, 3.76, 3.78, 3.80 MeV close to the transition temperature (thin lines), and their sum (thick line) obtained weighting evenly the different temperatures. Right: microcanonical distributions at energies spanning the coexistence region E/N = 0.75, 1.25, 1.75, 2.25, 2.75 MeV (thin lines), and their sum (thick line) obtained weighting evenly the different energies. The closest neighbors coupling is fixed to ε = 5.5 MeV.*

while if ρ is close to -1 it tends to a constant, but in no case the reweighting procedure applied to the monomodal distribution creates a spurious bimodality.

Another example of the effect of the reweighting procedure is given in Fig.5. The right part of Fig.5 shows microcanonical calculations within the lattice gas model[4]. Several distributions of the largest cluster size obtained for different total energies are displayed. In agreement with Fig.1, these distributions are never bimodal, even if the total energy interval is chosen such that the first order phase transition is crossed by the calculation. The bimodality is recovered if these distributions are summed up with equal weight following eq.(24) (thick line in Fig.5). The detailed shape of the reweighted distribution obviously depends on the energy interval used, a wider interval leading to an increased distance in energy between the maximum and the minimum.

For comparison, canonical distributions at different temperatures close to the transition temperature are displayed in the left part of the same figure. Because of the finite system size, the distributions are bimodal over a narrow but finite temperature range, while the transition temperature can be identified from the requirement that the two peaks have approximately the same height[4]. We can see that the canonical distribution close to the transition point is wider than the reweighted microcanonical one, and its concavity anomaly is more pronounced, however the shapes of the two distributions are very close. The width of the transition interval (i.e. the distance between the two peaks) as estimated from microcanonical calculations is a lower limit of the physical transition interval, and the quality of this estimation depends on the energy width of the available sample.

In the experimental case, due to the incomplete detection and the imperfect emission source selection, only an approximation of the deposited energy can be measured via measurable observables like transverse energy or calorimetric energy. We have checked that allowing a finite energy width does not change the result: an equal reweighting of gaussian ensembles leads to a distribution virtually identical to the one displayed in the right panel of Fig.5. An equal reweighting of canonical distributions is also shown in Fig.5: the resulting distribution is almost superposable to the distribution at the transition temperature.

These examples suggest that, if the microcanonical entropy presents a convexity, it may be possible to recognize it from the experimental data through a reweighting procedure, provided we dispose of an experimental sample sufficiently large in deposited energy.

A more challenging situation is given by the presence of a critical phenomenon. In this case a variation of the control parameter leads again the system to pass from one phase to another, but this transition is continuous and does not correspond to a convex microcanonical entropy. Fig.6 shows calculations performed within the bond-percolation model[27]. This model presents a critical behavior at a value p_c of the bond-breaking probability. As the Lattice gas model can be considered as a prototype for phase coexistence and first-order phase transitions, similarly the percolation model is the simplest realization of a second order phase transition. The percolation distribution close to the critical point is very close to the microcanonical lattice gas distribution in the middle of the coexistence region of the first-order transition. The consequence of this well-known feature[21, 22] is that it is still not clear whether nuclear-multifragmentation is better described as a critical phenomenon[28] or a first-order phase transition[29, 30].

Figure 6 shows that also in this case the presence of a phase transition is detected by the reweighting procedure: a flat
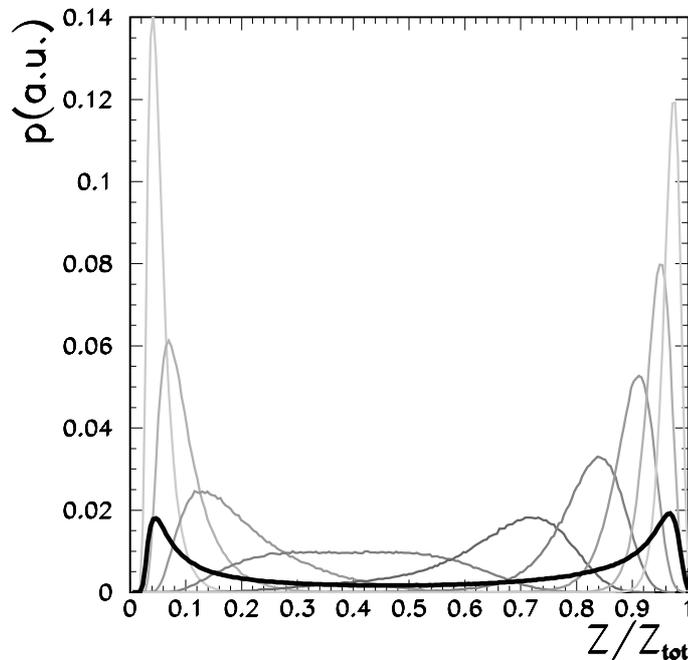
FIG. 6: *Calculations in the bond three-dimensional percolation model for a system of 216 particles. Thin lines: distribution of the size of the largest cluster for equally spaced values of the bond-breaking probability from $p = .16$ to $p = .56$ including the critical value p_c. Thick line: summed distribution obtained weighting evenly the different p's.*

distribution of bond-breaking probabilities leads to a global distribution qualitatively very similar to the distribution at the critical point if the p's interval is narrow, but if we have a sample including p's sufficiently far away from the critical probability as in Figure 6, two peaks appear corresponding to the ordered ($p \approx 0$) and disordered ($p \approx 1$) phase (thick line).

From Figure 5 and Figure 6 we can see that in both models the reweighted distribution show the presence of the two phases, with an important difference though. If the lattice-gas calculation shows a clear convexity between the two phases, associated to the convex intruder in the microcanonical entropy, this is not the case for the percolation distribution which, in the critical mass region, largely keeps the convexity of the critical point, i.e. it is essentially flat. This statement is quantified in Figure 7, which shows the numerically calculated first and second derivative of the reweighted distributions in the two models. Only the model associated to a first order phase transition exhibits a region of positive convexity.

This result can be easily understood. Indeed from eq.(24) we can identify the (inverse) curvature of the reweighted distribution with a (generalized) susceptibility:

$$\frac{\partial^2 \log p_w}{\partial Z^2} = \frac{\partial^2 S}{\partial Z^2} = \chi_\mu^{-1} \qquad (25)$$

The back-bending shown by the lattice gas calculation in Fig.7 has then the same physical meaning as the well-known back-bending of the microcanonical caloric curve[23], and allows to unambiguously identify a discontinuous (first order) phase transition.

B.   Application to experimental data

In the previous section we have seen that, for different model cases that can be relevant for nuclear multi-fragmentation, the concavity properties of the reweighted distribution reflect the concavity of the underlying entropy.

However we may wonder whether the different behaviors shown in Figs.3,4,5,6 will be distinguishable in realistic experimental cases, where distributions are often affected by important statistical as well as systematic error bars.

Even more important, we may also ask whether the behaviors of the schematic models we have shown can be taken as general representatives of the presence or absence of a first order phase transition. From a mathematical point of view, the two-dimensional function $\log p_w(x_1, x_2)$ is concave everywhere if and only if all the eigenvalues of the curvature matrix $c'_{ij} = \partial^2 \left(S(x_1, x_2) - S(x_1) \right) / \partial x_i \partial x_j$, are negative. A necessary and sufficient condition that an
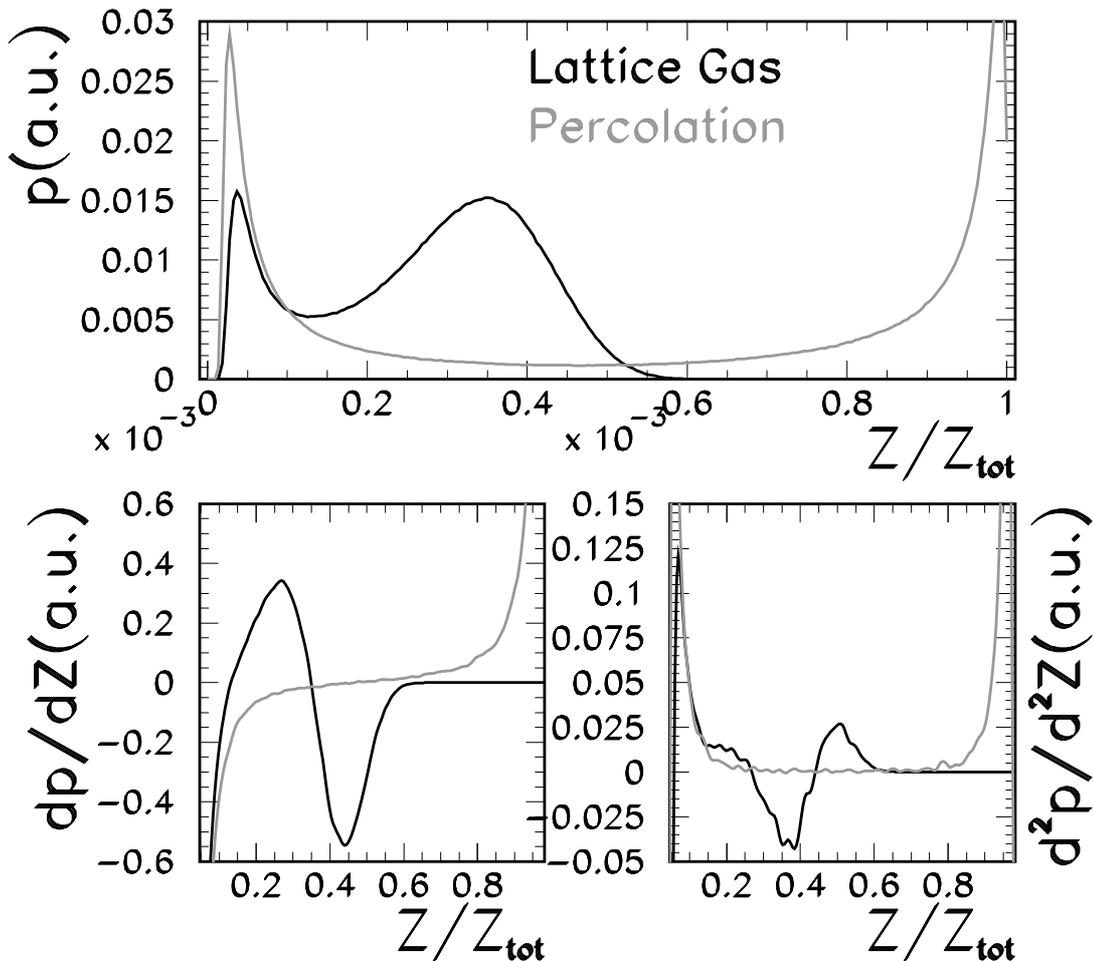
FIG. 7: *Upper part: reweighted distributions of the size of the largest cluster for a system of N=216 particles with the lattice gas and the percolation model. Lower part: first (left) and second (right) derivatives of the distributions.*

hermitian matrix has negative eigenvalues is that the minors of the determinant are negative, *i.e.*

$$c'_{11} \leq 0 \quad ; \quad detC' \leq 0$$

which in our case becomes

$$\frac{\partial^2 S(E,Z)}{\partial E^2} - \frac{\partial^2 S(E)}{\partial E^2} \leq 0 \quad ; \quad detC - \frac{\partial^2 S(E)}{\partial E^2}\frac{\partial^2 S(E,Z)}{\partial Z^2} \leq 0 \qquad (26)$$

for every (E, Z) value. In principle these conditions can be violated even if $S(E, Z)$ and $S(E)$ are concave everywhere. This means that we cannot a priori exclude a concave entropy even if we observe a bimodality in p_w.

In addition to that, only if a distribution is approximately symmetric we can visually judge, or numerically calculate, its convexity properties. In the experimental case, we may not dispose of an energy sample wide enough to construct a symmetric distribution around the transition value. It is clear for exemple that if in Figs.5, 6 we would sum up only low energy (respectively, low ps) samples, in both models a shoulder at low Z would be observed, and we would not be able to clearly discriminate between the first order and the second order scenario. This is probably the case in quasi-projectiles events, where the dynamics of the collision strongly favors low excitation energy deposit, and the desordered phase may barely, if ever, be attained[9].

To be conclusive about the presence of a first order phase transition we have therefore to show that the observed distribution is not compatible with a concave entropy, or in other words that a single saddle point approximation cannot explain the data as we have developed in section 4.

In realistic experimental cases this can be tested through a χ^2 test. Indeed in the absence of a phase transition

the underlying entropy is everywhere concave, a single saddle point approximation is reasonable, and the reweighted two-dimensional probability should be well described by:

$$p_w(E, Z) = \frac{W(E, Z)}{W(E)} = \frac{1}{\sqrt{2\pi\sigma_Z^2(1 - \rho^2)}} exp\left[-\frac{1}{2(1 - \rho^2)} \left(\frac{\rho}{\sigma_E}(E - E_0) - \frac{1}{\sigma_Z}(Z - Z_0) \right)^2 \right] \tag{27}$$

The parameters $E_0, Z_0, \sigma_E, \sigma_Z, \rho$ should be fitted to the experimental reweighted distribution. A χ^2 test should allow to exclude the adequacy of the fit.

If fragmentation events are compatible with a critical phenomenon, both the single and the double saddle point approximation should fail. This means that in this scenario we should not be able to describe the data with the reweighted single gaussian eq.(27), not with the reweighted double gaussian. An application of this method to INDRA data is in progress[11].

VI. CONCLUSIONS

In this paper we have critically analyzed the bimodality observable proposed in [2] to track a first order phase transition, which has been extensively used to analyze multi-fragmentation data[8, 9, 10, 11, 12]. We have shown that the out-of-equilibrium dynamics of the entrance channel, as well as the different data sorting conditions, can bias the signal in an uncontrolled way, tending to suppress the bimodal behavior. Based on the correlation between the bimodality observable and the deposited energy, we propose a reweighting method on the measured distributions, with the aim of disentangling the dynamic dissipation properties from the entropy characteristics. This method applied on different schematic models, is seen to provide an excellent discrimination between the case of a first-order phase transition, a critical phenomenon and the absence of transition. A chi-square test is proposed for the experimental case to demonstrate/refute the existence of a convexity in the microcanonical entropy.

[1] K. Binder and D. P. Landau, Phys. Rev. B **30**, 1477 (1984).
[2] Ph. Chomaz, F. Gulminelli and V. Duflot, Phys. Rev. E **64**, 046114 (2001).
[3] K.C. Lee, Phys. Rev. E **53**, 6558 (1996) ; Ph. Chomaz and F. Gulminelli, Physica A **330**, 451 (2003).
[4] F.Gulminelli, Ann. Phys. Fr. **29** (2004) 6, and references therein.
[5] R. Botet, M. Ploszajczak, Phys.Rev. E **62**, 1825 (2000).
[6] "'Dynamics and thermodynamics with nuclear degrees of freedom"', P.Chomaz et al eds, Eur.Phys.Journ. A **30**, Springer III (2006).
[7] J. B. Elliott, et al., Phys.Rev.Lett. **88**, 042701 (2002).
[8] N. Bellaize et al., Nucl. Phys. A **709**, 367 (2002).
[9] M. Pichon, et al., Nucl.Phys. A **779**, 267 (2006).
[10] B. Borderie, J. Phys. G. **28**, R217 (2002); M. Rivet, et al., Nucl.Phys. A **749**, 73 (2005).
[11] E.Bonnet, PhD Thesis, IPN (2006), http://tel.ccsd.cnrs.fr/tel-0000; E.Bonnet et al., in preparation.
[12] P. Lautesse et al., Phys. Rev. C **71**, 034602 (2005).
[13] R. Botet, M. Ploszajczak et al. Phys. Rev. Lett. **86**, 3514 (2001).
[14] J.D. Frankland et al., Phys. Rev. C **71**, 034607 (2005); J. D. Frankland et al, Nucl. Phys. A **749**, 102 (2005).
[15] N.Le Neindre et al., to be published.
[16] F. Gulminelli , J.Carmona, Ph.Chomaz, J.Richert, S.Jimenez, V.Regnard, Phys.Rev.E **68**, 026119 (2003).
[17] P. Labastie and R. L. Whetten, Phys. Rev. Lett. **65**, 1567 (1990).
[18] H. Reinhardt, Nucl. Phys. A **413**, 475 (1984); R. Balian, Y. Alhassid, H. Reinhardt, Phys. Rep. **131**, 1 (1986).
[19] Ph.Chomaz and F.Gulminelli, Eur.Journ.Phys. A **30**, 317 (2006).
[20] F. Bouchet, J. Barré, Journ. Stat. Phys. **118**, 1073 (2005), and references therein.
[21] J.Carmona et al, Nuclear Physics A **643**, 115 (1998).
[22] Ph.Chomaz, F.Gulminelli, Physical Review Letters **82**, 1402 (1999); F.Gulminelli et al, Phys.Rev.C **65**, 051601 (2002); F.Gulminelli,Ph.Chomaz, Physical Review C **71**, 054607 (2005).
[23] D. H. E. Gross, "Microcanonical thermodynamics: phase transitions in finite systems", Lecture notes in Physics vol. **66**, World Scientific (2001).
[24] R.Balian, 'From microphysics to macrophysics', Springer Verlag (1982).
[25] M. S. Challa, J. H. Hetherington, Phys. Rev. Lett. **60**, 77 (1988) and Phys. Rev. A **38**, 6324 (1988).
[26] F. Gulminelli, Ph. Chomaz, Europhys. Lett. **50**, 434 (2000).
[27] D.Stauffer and A.Aharony, "'Introduction to Percolation Theory"', 2nd ed., Taylor and Francis, London (1994).
[28] X. Campi, H. Krivine, E. Plagnol, N. Sator, Phys.Rev. C **67**, 044610 (2003).

[29] M.D'Agostino et al, Physics Letters B **473**, 219 (2000); M.D'Agostino et al, Nuclear Physics A **734**, 512 (2004).
[30] M.Bruno et al., ArXiv:nucl-ex/0612030